

Simulation of Be armour cracking under ITER-like transient heat loads



S. Pestchanyi^{a,*}, B. Spilker^b, B. Bazylev^a

^a Karlsruhe Institute of Technology, INR, Hermann-von-Helmholtz-Platz 1, Eggenstein-Leopoldshafen, 76344, Germany

^b Forschungszentrum Jülich GmbH, Institut für Energie- und Klimaforschung, 52425 Jülich, Germany

ARTICLE INFO

Article history:

Received 9 November 2015

Revised 4 March 2016

Accepted 6 June 2016

Available online 16 June 2016

Keywords:

Beryllium

Cracking

Numerical simulation

JUDITH 1

ITER

ABSTRACT

Simulation of beryllium cracking under action of multiple severe surface heatings has been performed using the PEGASUS-3D code and verified by experiments in the JUDITH 1 facility. Analysis of the results has revealed beryllium thermo conductivity degradation under action of repetitive pulsed heat load due to accumulation of the cracks in the surface layer. Thermo conductivity degradation is found to be at least 4 times after 100 pulses in JUDITH 1 facility. An analytical model for the Be cracking threshold under action of arbitrary heat pulses has been developed.

© 2016 The Authors. Published by Elsevier Ltd.
This is an open access article under the CC BY-NC-ND license
(<http://creativecommons.org/licenses/by-nc-nd/4.0/>).

1. Introduction

Beryllium is foreseen as the reference armour material for the first wall in ITER because of its high thermal conductivity and low atomic number Z. Special high heat load tests performed with Be have proven its applicability for normal operation of ITER. However, its behaviour during off-normal events like disruptions, mitigated disruptions, and ELMs, when the heat flux to the armour increases by orders of magnitude, still needs accurate evaluation.

Disruptions are unavoidable crashes of the tokamak discharges, which deposit the plasma energy and the poloidal magnetic field energy onto the plasma facing components of the tokamak vacuum vessel. Disruptions happen regularly in modern tokamaks, but the first wall damage due to the disruptions is negligible because of moderate energy content in the hot core of these tokamaks. However, an unmitigated disruption in the future tokamak ITER will probably damage the first wall of its vacuum vessel, causing significant melting and even vaporization. This is why a special disruption mitigation system (DMS) has been proposed for ITER. DMS prevents direct contact of the hot core plasma with the Be armour, thus mitigating the armour damage, but it increases radiation heat load to the wall. Nevertheless, the radiation heat flux can cause cracking of the armour or even surface melting [1, 2]. Severe and deep melting of Be armour should be avoided, but smaller ITER events, without melting or with shallow melting and re-solidification of a few microns, could be tolerable.

Beryllium cracking and melting under action of ITER-like transients have been investigated experimentally [3–7]. However, understanding of the cracking mechanism and its consequences for Be armour lifetime are not investigated at all. This paper mainly devoted for investigation of the mechanisms and influence of cracking on Be properties as well as for experimental validation of the results obtained. Special series of experiments on Be specimens which apply high heat loads at the surface generated by an electron beam have been performed in the JUDITH 1 facility. The parameters of heat loading in JUDITH 1 have been chosen to simulate ITER first wall armour loading during mitigated disruptions and ELMs. Analysis of the crack pattern on the surface and penetration of the crack into the bulk has been done. Investigation of the Be armour cracking simulating the conditions of JUDITH 1 experiments has been performed using the PEGASUS-3D code [8–12]. Comparison of the experimental and the simulation results has been performed for validation of the PEGASUS-3D simulations and for prediction of Be cracking under ITER conditions using this code.

2. Simulation of transient loads on Be in the JUDITH 1 facility

The experimental simulation of the thermal shocks has been performed in the electron beam facility JUDITH 1 (Juelich Diverter Test Facility in the Hot Cells) [13]. All tested samples were polished with 1 μm diamond suspension to guarantee a well-defined pristine initial state before the testing. The electron beam has full width at half maximum (FWHM) of ~ 1 mm and is swept over the loaded area of the samples with frequencies of 40 kHz and 31 kHz in the y and z directions along the surface, respectively. The samples were kept at room temperature during the thermal

* Corresponding author.

E-mail address: serguei.pestchanyi@kit.edu (S. Pestchanyi).

shock exposure. The pulse duration for all applied thermal shock pulses was 1 ms, which is the minimum possible pulse duration of JUDITH 1. Furthermore, power densities of up to 900 MW/m² were applied, taking into account the size of the loaded area and the electron absorption coefficient of beryllium 0.99, determined by Monte-Carlo simulations. The acceleration voltage was 120 kV. The loading frequency of 0.5 Hz was sufficiently low to enable a complete cool-down of the samples to the equilibrium room temperature between two thermal shock pulses. On different samples, pulse numbers of 1, 10, 100, and 1000 were applied.

Subsequently, the exposed samples were investigated by means of scanning electron microscopy and laser profilometry. Following the non-destructive analysis methods, the samples were cut perpendicular to the loaded area with a diamond saw and ground/polished down to the centre of the loaded area and chemically etched. This metallographic cross sectioning revealed the extent of damages and cracks from the loaded surface down into the bulk material.

A series of experiments have been performed applying 100 pulses of 1 ms duration with the power densities of 200, 400, 500, 600, 700, 800, 900 MW/m². These experiments have revealed that the targets surface melting starts at 900 MW/m². At 800 MW/m² Be target shows cracks only. Separate cracks arise at 400 MW/m², while at 200 MW/m² the cracks are absent at the sample surface. Loading with increasing power densities 500 800 MW/m² resulted in increasing the number of cracks and the crack average width.

Second series of experiments have been performed applying 1, 10, 100 and 1000 pulses with the power density of 900 MW/m² of 1 ms duration to different target spots. The results of these experiments have shown that no cracks appear after 1 pulse. After 10 pulses the cracks appears at the corners and in the centre of the Be target with average width of $W \sim 5\text{--}7\ \mu\text{m}$ and average distance between the cracks of $D \sim 200\text{--}400\ \mu\text{m}$. The results of the experiments are illustrated in Figs. 1–3.

3. Numerical simulation of the JUDITH 1 experimental results

3.1. Simulation of power deposition from JUDITH 1 electron beam in Be

The volumetric energy depositions by electrons accelerated in JUDITH 1 facility into Be target has been calculated by the Monte Carlo code ENDEP. The Monte Carlo model describing propagation of charged particles inside materials is based mainly on the pair collisions approximation. Long distance electron-electron interactions are taken into account statistically in frame of multiple-scattering model. The following processes are included in the Monte Carlo model: 1) electron-electron scattering, 2) electron-electron collisions (long distance), 3) electron-nuclear scattering, 4) Bremsstrahlung, 5) Compton scattering, 6) Auger processes, 7) photo ionization and recombination, 8) electron and photon avalanche simulations. Most features of the Monte Carlo model are described in detail in [14]. The result of the simulation is shown in Fig. 4. According to the simulation, all the heating power is deposited inside the surface layer of $\sim 110\ \mu\text{m}$, the distribution maximum is at $64\ \mu\text{m}$.

For the numerical simulations of the JUDITH 1 experiments with power deposition onto the samples of 1 cm thickness placed on metallic plates exposed by 120 keV electron beam in scanning mode are considered. The pulse duration τ has been set to 1 ms; the loaded surface was limited to $4 \times 4\ \text{mm}$. The fast electron beam scanning regime with frequencies $f_y = 40\ \text{kHz}$ and $f_z = 31\ \text{kHz}$ has been simulated using the MEMOS code [15]. The electron beam power has exponential profile with FWHM of 1 mm. Resulting power deposition pattern and the scanning beam trajectory are shown in Fig. 5. Averaged over 1 ms space distribution for the heat

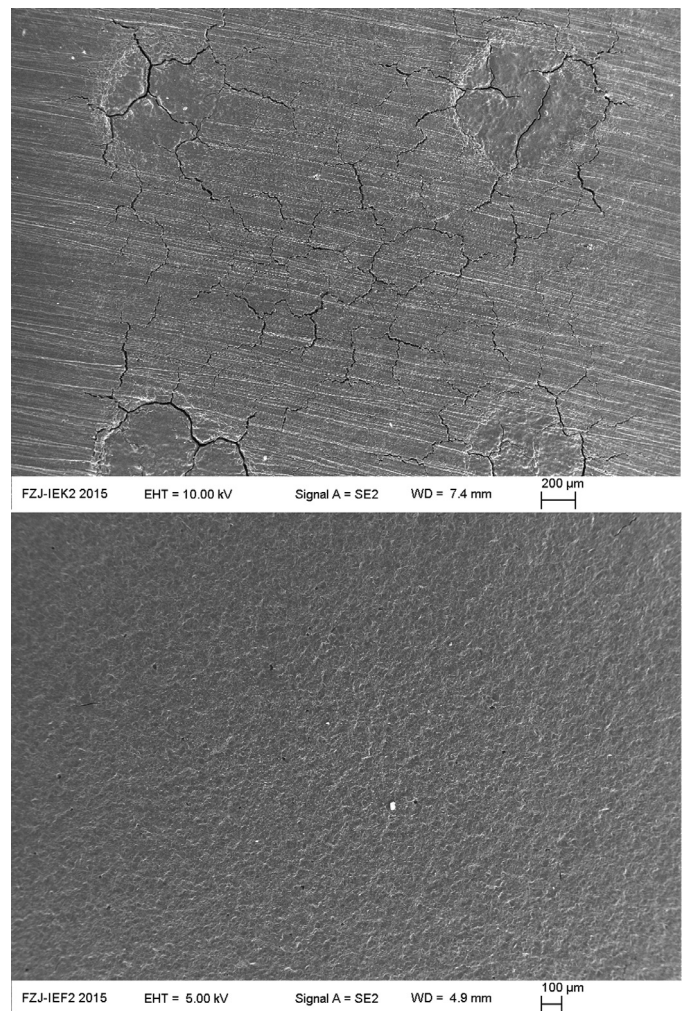


Fig. 1. Be samples surface after irradiation in JUDITH. The surface melting starts at 900 MW/m², after 100 pulses of 1 ms duration (upper panel). At 800 MW/m², after 100 pulses Be shows cracks only (lower panel).

flux from the JUDITH 1 electron beam looks uniform enough inside the $4 \times 4\ \text{mm}$ spot to use uniform power deposition for the cracking simulation in PEGASUS-3D code.

3.2. Simulation of the experimental results using the PEGASUS-3D code

Simulation of the JUDITH 1 experimental results with the PEGASUS-3D code has been performed using the temperature dependent thermo-physical parameters from [16,17]. The simulations have revealed that surface melting should start at the electron beam power density equal to 1100 MW/m² in contrast with the experimental observation of surface melting at 900 MW/m². Some hints for resolving this contradiction have been found in the melt layer pattern at the Be sample surface. One can see from Fig. 1 that the melt spots arise at the corners of the irradiated region. The first explanation for the effect could be inhomogeneity of the heating by the scanning electron beam. However, simulation of the power deposition onto Be plate (Chapter 3.1) has confirmed rather good homogeneity of the time averaged heat flux, see Fig. 5.

Further simulations have revealed that averaging of the electron beam heat flux over time intervals, smaller than 1 ms, shows rather large peaks on the heating flux distribution. For example, Fig. 6 illustrates the heat flux averaged over sequential time

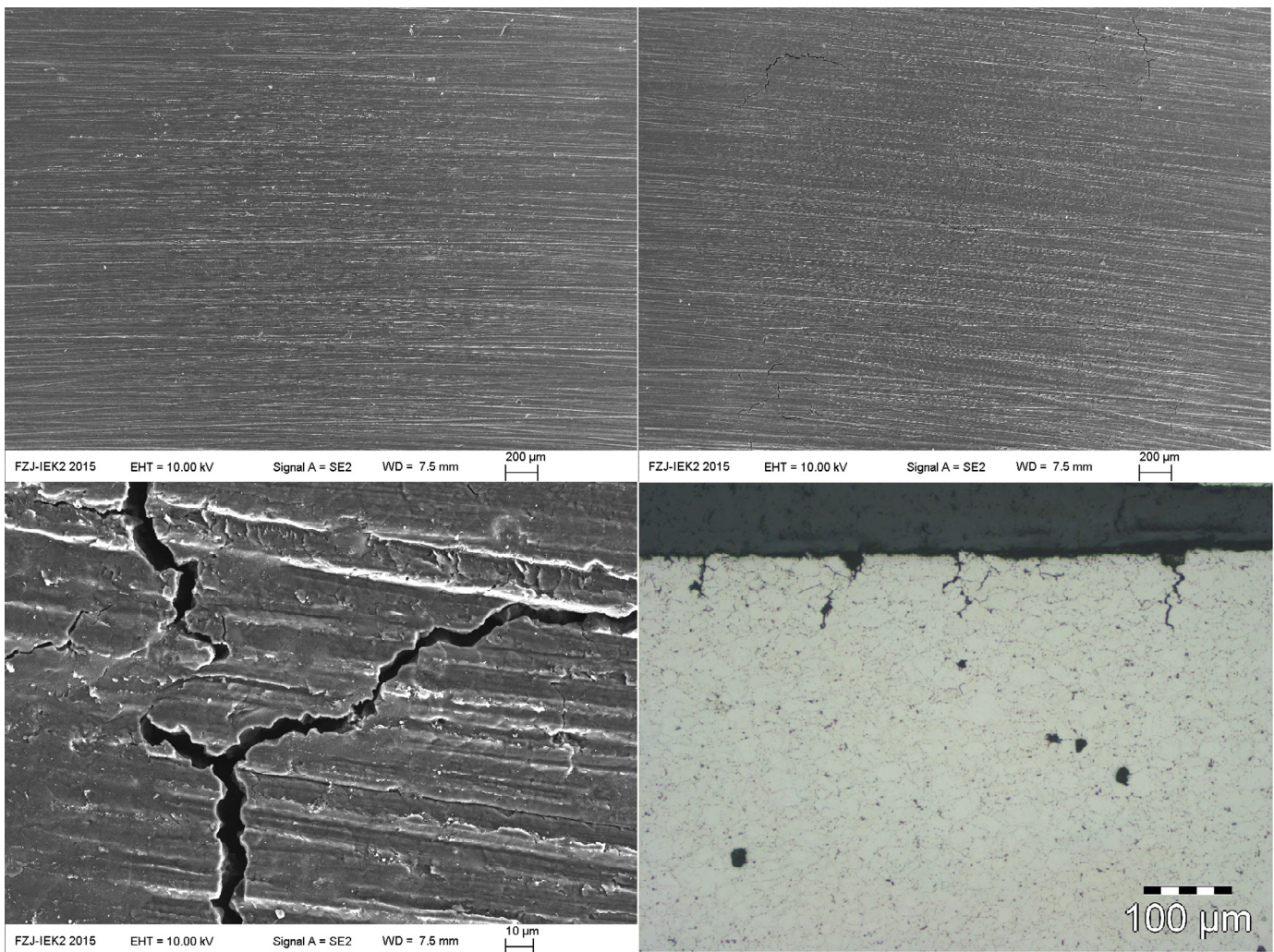


Fig. 2. Cracking of Be target under exposure at 900 MW/m^2 pulses of 1 ms duration: no cracks after 1 pulse (upper left panel). After 10 pulses the cracks appears at the corners and in the centre with average width of $W \sim 57 \mu\text{m}$ and average distance between the cracks of $D \sim 200400 \mu\text{m}$. View from top on the cracks at the sample surface (upper right), close view on the surface cracks (lower left) and the cross section through the cracked sample (lower right).

intervals of 0.2 ms. The ratio of the heat flux maxima (at the corners) to the flux minimum reaches up to two times. This large time variation has been taken into account in the PEGASUS-3D simulations. For example, real time dependence of the heat flux at the corner position ($y = 1 \text{ mm}$, $z = 1 \text{ mm}$), where melting starts is much more irregular than the flux at the intermediate position ($y = 1 \text{ mm}$, $z = 2 \text{ mm}$), where no melting exist at the average heat flux of 900 MW/m^2 , see Fig. 7.

Simulation of the Be sample heating using the real time dependence for the heat flux at the corner, shown in Fig. 7 have resulted in maximum surface temperature of 1380 K, which is much lower than the Be melting temperature 1560 K. The only way to explain the melting of the Be at the corners of the irradiated spot is to assume degradation of its thermo conductivity due to accumulation of cracks inside Be sample under the heated surface. The effect of thermo conductivity degradation has been investigated earlier for the fine grain graphites in [18]. Using numerical simulations with PEGASUS-3D code, it has been shown in this paper that the effective thermo conductivity of a sample with cracks can degrade up to one order of the magnitude with increasing the density of cracks in the bulk material. Experimental demonstration of the cracks influence on the thermo conductivity has been detected in the plasma gun experiments [19]. The thermo conductivity in the thin surface

layer of the sample with cracks has been found to be at least 4 times lower than the thermo conductivity of virgin material. The cracks in the surface layer and hence the degradation of thermo conductivity appeared after multiple surface heating with plasma shots in the plasma gun.

Assuming the same mechanism of the thermo conductivity degradation for Be one may conclude that melting of the sample surface at 900 MW/m^2 has been determined by accumulation of cracks under the sample surface during 100 shots in the JUDITH 1 facility. A parametric study of heating the Be sample with degraded thermo conductivity has revealed that, assuming the degradation coefficient is of 0.25, one can explain the experimental results. In this case the Be sample melts at the corners and does not melt in between, as it has been observed in experiment.

For verification of these deductions, a dedicated series of additional experiment has been performed in the JUDITH 1 facility. In these experiments virgin Be target has been loaded with 1 and 10 pulses of power density in the range $1000 \text{--}1300 \text{ MW/m}^2$. In these experiments the first traces of the virgin Be melting have been found at 1300 MW/m^2 after 1 shot. This finding confirms that the thermo-physical data for the virgin Be without cracks, used in the simulations are in reasonable agreement with experiment. After 10 shots Be melts at all the power densities in the range.

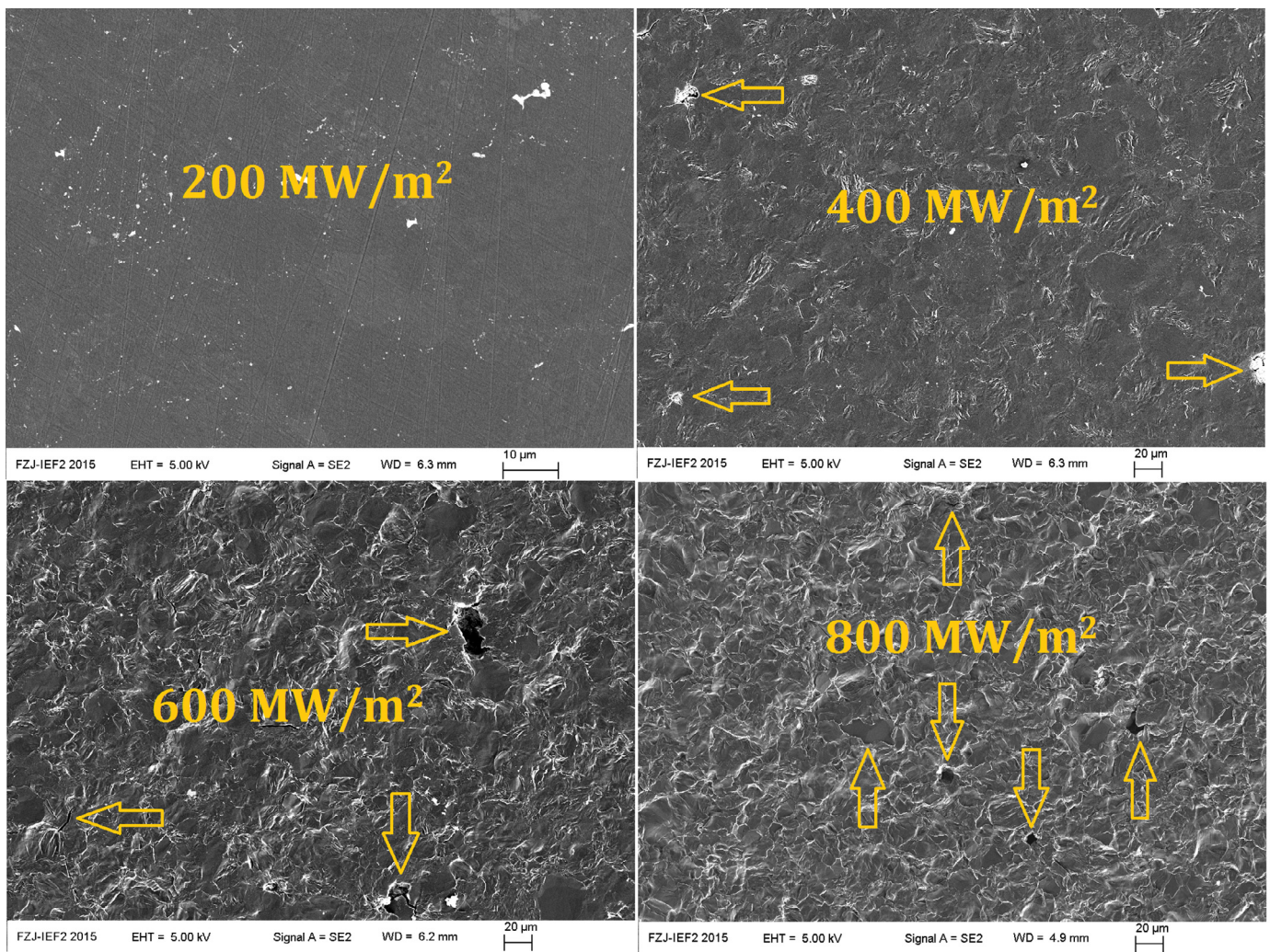


Fig. 3. Be target cracking under action of 100 pulses of 1 ms duration in JUDITH 1 facility. The cracks are indicated with arrows. Separate cracks arise at 400 MW/m², and develop with growing heat load, while at 200 MW/m² the cracks are absent at the sample surface.

3.3. Cracking threshold for Be

Tungsten cracking under influence of severe heating by type I ELMs in ITER has already been investigated using the PEGASUS-3D code [20]. Tungsten and beryllium have similar cracking properties due to the fact, that thermal expansion coefficients for both are large enough to produce thermo stress value much larger than the yield stress, when heated to temperatures, comparable with the melting temperature. This cause plastic deformation of the heated surface, which in turn lead to cracks formation. The cracking mechanism, which will be described below is general for all ductile metals, so it would be reasonable to apply it to beryllium. The cracks arise in thin heated surface layer due to tensile stress. The mechanism of the tensile stress generation is as follows.

During surface heating the stress developed in thin surface layer of solid target is compressive due to thermal expansion under action of heating. If compression during the heating is elastic then, during cooling down, the compressive stress fully relaxes and deformation is absent, so cracks do not appear. However, if the compressive thermo stress exceeds the yield strength during heating, then the surface layer is plastically deformed: it compressed along the surface and expanded in perpendicular direction. During cooling down of the plastically deformed layer the compressive stress relaxed at the temperature, higher than the initial temperature due to the plastic deformation. Then, during further cool-

ing down, a tensile stress is developed in the plastically deformed surface layer due to its interaction with the undistorted bulk material. If this tensile stress exceeds the tensile strength, then the crack is generated at the surface. Summarizing, one can say, that the main mechanism of tungsten cracking is compressive plastic deformation of the tungsten surface under action of compressive thermo stress followed by development of tensile stress inside the deformed surface layer in the course of the cooling down after the heating pulse. The cracks at the heated tungsten surface are produced by the tensile stress at the end of cooling down phase after the heating stops.

Assuming the same cracking mechanism for Be one can roughly estimate the cracking threshold from simplified 1D model with static boundary conditions using thermo-physical properties of beryllium. First of all, one should note that cracking of Be due to short severe heating close to the cracking threshold starts after several (possibly several thousands) pulses. If the heat flux is above the cracking threshold then Be surface is heated to the temperature, which provides the compressive stress σ , higher than the yield stress σ_y . This stress plastically deforms the surface layer to some value of deformation ε_p , which depends on the heating power. After cooling to intermediate temperature, when the surface stress relaxed $\sigma = 0$, the residual deformation is $\varepsilon = \varepsilon_p$. During further cooling down a tensile residual stress is developed in the heated surface layer, which approximately equal to $\sigma_r = -\varepsilon E$, E

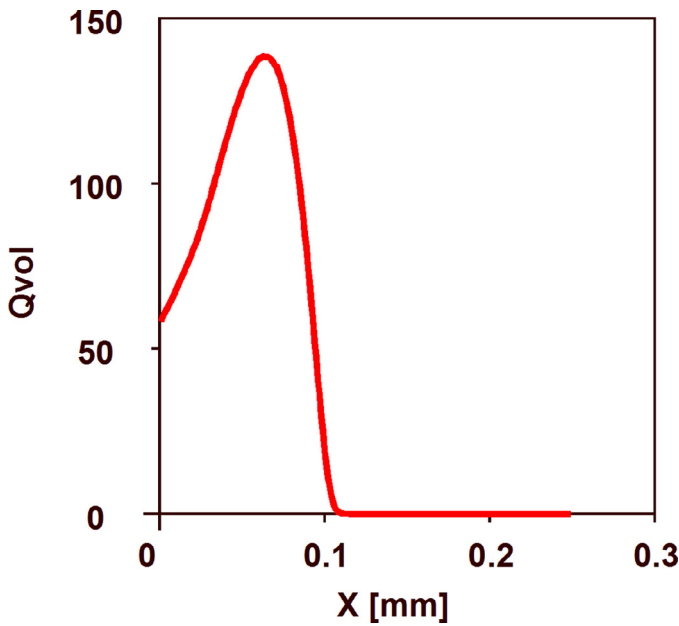


Fig. 4. Power deposition inside the Be target from electron beam in the JUDITH 1 facility with 120 keV electrons energy. The distribution is normalized by condition $\int_0^\infty Q_{vol}(x)dx = 1$. The target surface corresponds to $x=0$. The $Q_{vol}(x)$ maximum is at $x=0.064$ mm.

the start of cracking:

$$T_{th} - T_0 \cong \frac{\sigma_y(T_{th}) + \sigma_u(T_{th})}{E(T_{th})\alpha(T_{th})}$$

Substituting the thermo-physical parameters of Be one can find that $T_{th} - T_0 \approx 200$ K. This value is noticeably lower than the temperature rise of 494 K, simulated with the PEGASUS-3D code for the shots of 400 MW/m², where cracking has been found in the experiment and even lower than 256 K rise, calculated for 200 MW/m² pulses, where cracking is not experimentally detected after 100 pulses. The threshold power density value for Be cracking in the JUDITH 1 facility, calculated with the PEGASUS-3D code, corresponds to ~ 160 MW/m². This contradiction is similar to the contradiction between calculated and measured tungsten cracking threshold values, investigated earlier [21]. For tungsten the cracking threshold has also been estimated to be 3 times smaller than the value, registered in experiments with few hundred shots, but later on this small threshold value has been found in experiment with 1 million shots, applied to the tungsten surface [21,22]. One should expect similar effect for Be, but the estimated threshold value should be verified by experiment.

4. Conclusions

Simulation of beryllium cracking under action of multiple severe surfaces heating has been performed using the PEGASUS-3D code and verified by the dedicated series of experiments in the JUDITH 1 electron beam facility. Several series of experiments have been performed in the JUDITH 1 facility for verification of the numerical simulation results and for verification of the thermo-physical properties used.

Analysis of the experimental results and their comparison with the simulations has been performed. The simulations have predicted surface melting start at the power density equal to 1100 MW/m² in contrast with the experimental observation of surface melting at 900 MW/m². Analysis of this contradiction has revealed that the heat flux in JUDITH 1 facility considerably differ from uniform and constant in time due to the electron beam scanning. However, using the real heat flux with scanning for simulations did not eliminate this contradiction though decreased the difference. Further analysis has revealed that the experimental results testify for the beryllium thermo conductivity degradation under action of repetitive pulsed heat load. Degradation of the thermo conductivity at least 4 times after 100 pulses of 900 MW/m² has been found.

Summarizing, one can explain, that Be cracking starts at corners of the loaded spot due to inhomogeneity and time variability of heating by electron beam scanning. Besides, measured value of the melting threshold can be explained by thermo conductivity degradation due to accumulation of the cracks in the surface layer. Thermo conductivity degradation under action of repetitive ELMS influences Be armour lifetime, so it will be studied in details in future investigations.

An analytical model for the Be cracking threshold under action of arbitrary heat pulses has been developed. The model predicts that the surface cracking under the JUDITH 1 conditions should start at the threshold power density value of ~ 160 MW/m². The threshold power density value, measured in the JUDITH 1 facility after 100 pulses is between 200 MW/m² and 400 MW/m². The model predicts that the calculated threshold value should be measured in experiment with increased number of pulses. The experiment on verification of the calculated cracking threshold for Be is planned.

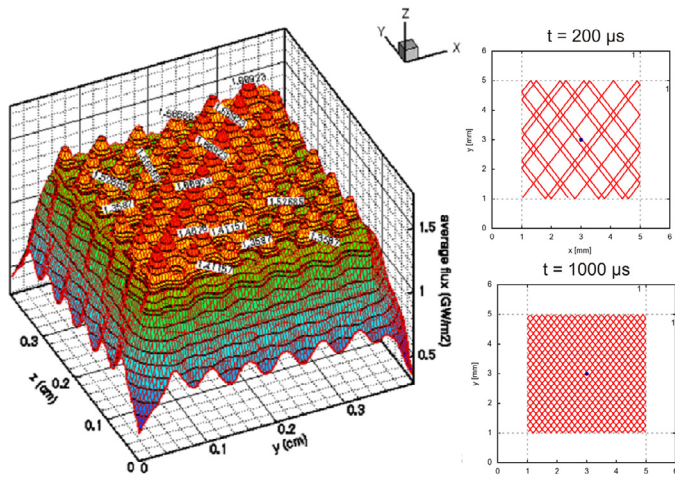


Fig. 5. Averaged over 1 ms space distribution for the heat flux from the JUDITH 1 electron beam (left panel) and the scanning beam trajectory at 0.2 ms and 1 ms (right panel). Scanning is with frequencies of 40 kHz and 31 kHz along the y- and the z-axis correspondingly. The starting point is $y=0$, $z=0$, scanning duration $\tau = 1$ ms, irradiated area is 4×4 mm.

is the Young's modulus. For accurate calculation of the stress, acting in the surface layer one should solve the equilibrium equations of Elasticity Theory, which is quite challenging. But for our calculations this approximate analytical estimation is enough. At the next pulse for start of the plastic deformation one should ensure stress of $\sigma \geq \sigma_y + \sigma_r$, even if we do not take into consideration the cold working. After n pulses the plastic deformation is $\varepsilon = n\varepsilon_p$, the residual tensile stress is $\sigma_r = -n\varepsilon E$. Again, for the next plastic deformation one should ensure the stress of $\sigma \geq \sigma_y + \sigma_r$. If, at some n , this residual stress exceeds the tensile strength σ_u of Be then it cracks. So, to accumulate the plastic deformation, which provides cracking, one should ensure the thermostress of $\sigma = \sigma_y + \sigma_u$. From this condition one can estimate the threshold temperature T_{th} for

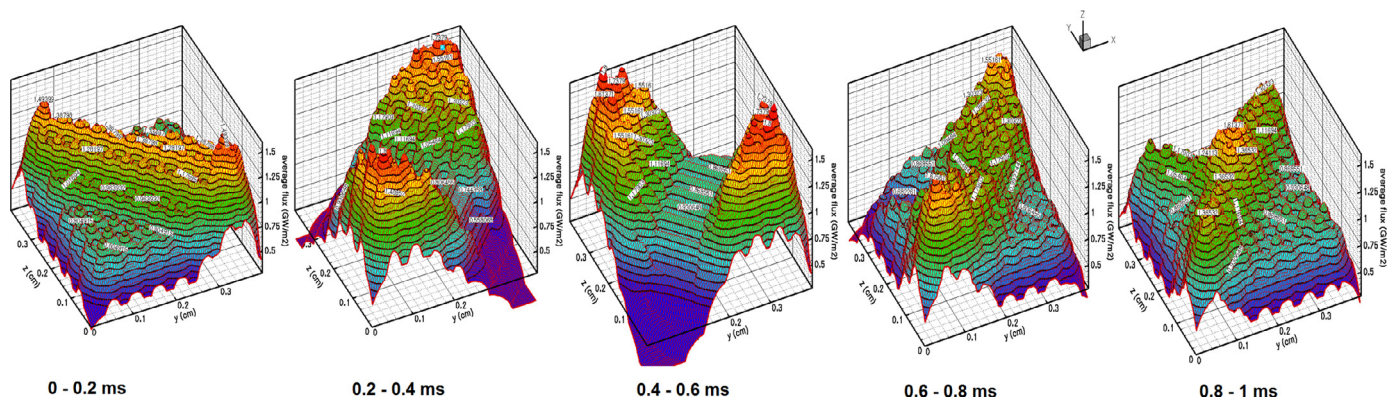


Fig. 6. Space distribution for the heat flux from the JUDITH 1 electron beam averaged over sequential time intervals of 0.2 ms. The averaging time intervals are indicated above the corresponding plots. The ratio of the heat flux maxima (at the corners) and the flux minimum reaches up to two times (see the plot for averaging interval 0.4–0.6 ms).

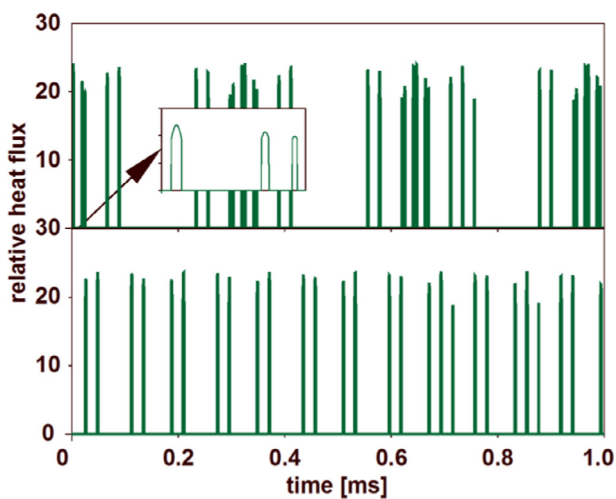


Fig. 7. Time dependence for the JUDITH 1 electron beam heat flux at two positions inside the heated spot of 4×4 mm. Upper panel corresponds to the corner position ($y = 1$ mm, $z = 1$ mm), where melting starts; lower panel – to the intermediate position ($y = 1$ mm, $z = 2$ mm), where no melting exist at the average heat flux of 900 MW/m^2 . Shown are relative heat fluxes, reduced on the average heat flux. The insert shows time dependence of the heat flux at the corner during first 0.013 ms with better time resolution.

Acknowledgement

This work was supported by Fusion for Energy agency and carried out within the framework of the contract F4E-OPE-584. The views and opinions expressed herein do not necessarily reflect those of F4E.

References

[1] N.S. Klimov, A.B. Putrik, J. Linke, et al., Plasma facing materials performance under ITER-relevant mitigated disruption photonic heat loads, *J. Nucl. Mater.* 463 (2015) 61–65.

[2] I. Kupriyanov, N. Porezanov, G. Nikolaev, et al., Study of beryllium damage under ITER-relevant transient plasma and radiative loads, *Fusion Sci. Technol.* 66 (2014) 171–179.

[3] G. Pintsuk, W. Kuhnlein, J. Linke, M. Rodig, Investigation of tungsten and beryllium behaviour under short transient events, *Fusion Eng. Des.* 82 (2007) 1720–1729.

[4] M. Rödig, R. Duwe, J. Linke, A. Schuster, High heat flux tests on beryllium and beryllium-copper joints, *Fusion Eng. Des.* 37 (1997) 317–324.

[5] M. Roedig, I. Kupriyanov, J. Linke, X. Liu, Zh. Wang, Simulation of transient heat loads on high heat flux materials and components, *J. Nucl. Mater.* 417 (2011) 761–764.

[6] I.B. Kupriyanov, Status of RF beryllium characterization for ITER fist wall, *J. Nucl. Mater.* 417 (2011) 756–760.

[7] IgorB. Kupriyanov, NicolayP. Porezanov, GeorgyiN. Nikolaev, Effect of transient heating loads on beryllium, *Fusion Eng. Des.* 89 (2014) 1074–1080.

[8] S. Pestchanyi, H. Wuerz, Brittle destruction of carbon based materials under off-normal ITER-FEAT conditions, *Phys./Scr.* 377 T91 (2001) 84–89.

[9] S. Pestchanyi, J. Linke, Simulation of cracks in tungsten under ITER specific heat loads, *Fusion Eng. Des.* 83 (15–24) (2007) 1657–1663.

[10] S.E. Pestchanyi, I.S. Landman, Simulation of Dust Production in ITER Transient Events, *Fusion Eng. Des.* 83 (2008) 1054.

[11] S. Pestchanyi, et al., *Fusion Eng. Des.* 85 (2010) 1697–1701 (plasticity).

[12] S. Pestchanyi, V. Makhilaj, I. Landman, Specific features of mechanism for dust production from tungsten armor under action of ELMs, *Fusion Sci. Technol.* 66 (2014) 150–156.

[13] R. Duwe, et al., *Fusion Technol.* 1 (1995) 355–358.

[14] G. Myloshevsky, H. Würz. 3-D Monte Carlo Calculations of Energy Deposition of Electrons into Bulk Graphite and into an Inhomogeneous Carbon Plasma Shield. Report FZKA 6482, Forschungszentrum Karlsruhe 2000.

[15] B.N. Bazylev, Y. Koza, I.S. Landman, J. Linke, S.E. Pestchanyi, H. Wuerz, Energy Threshold of Brittle Destruction for Carbon-Based Materials, *Physica Scripta.* T111 (2004) 213–217.

[16] ITER Materials Properties Handbook (MPH), ITER Doc. G 74 MA 16 04-05-07 R0.1

[17] <http://www-ferp.ucsd.edu/LIB/PROPS/PANOS/be.html>

[18] S.E. Pestchanyi, I.S. Landman, Effective thermal conductivity of graphite materials with cracks, *Physica Scripta.* T111 (2004) 218–220.

[19] S. Pestchanyi, I. Landman, Experimental verification of FOREV-2D simulations for the plasma shield, *J. Nucl. Mater.* 390–391 (2009) 822–825.

[20] S. Pestchanyi, I. Garkusha, I. Landman, Simulation of tungsten armour cracking due to small ELMs in ITER, *Fusion Eng. Des.* 85 (2010) 1697–1701.

[21] S. Pestchanyi, I. Garkusha, I. Landman, Simulation of residual thermostress in tungsten after repetitive ELM-like heat loads, *Fusion Eng. Des.* 86 (2011) 1681–1684.

[22] Th. Loewenhoff, J. Linke, G. Pintsuk, C. Thomser, Tungsten and CFC degradation under combined high cycle transient and steady state heat loads, *Fusion Eng. Des.* 87 (2012) 1201–1205.